EPJ Web of Conferences **274**, 04013 (2022) https://doi.org/10.1051/epjconf/202227404013
XVth Quark Confinement and the Hadron Spectrum

Heavy quark dynamics in a strongly magnetized medium

Aritra Bandyopadhyay[1,2,3,*], *Jinfeng* Liao[2,], and *Hongxi* Xing[3,]

[1]Institut für Theoretische Physik, Universität Heidelberg, Philosophenweg 16, 69120 Heidelberg, Germany
[2]Physics Department and Center for Exploration of Energy and Matter, Indiana University, 2401 N Milo B. Sampson Lane, Bloomington, IN 47408, USA
[3]Guangdong Provincial Key Laboratory of Nuclear Science, Institute of Quantum Matter, South China Normal University, Guangzhou 510006, China

Abstract. We present a calculation of the heavy quark momentum diffusion coefficients in a strongly magnetized medium, within the Lowest Landau Level (LLL) approximation. In particular, we use the Hard Thermal Loop (HTL) resummed effective gluon propagator, generalized for a hot and magnetized medium. Using this effective HTL gluon propagator along with the LLL quark propagator we analytically derive the full results for the longitudinal and transverse momentum diffusion coefficients for charm and bottom quarks beyond the static limit. Going beyond the static limit of the heavy quark, we also show numerical results for these coefficients in two special cases where the heavy quark is moving either parallel or perpendicular to the external magnetic field.

1 Introduction

Strong external magnetic fields are found to be present in some stellar objects [1] (e.g. neutron stars, anomalous X-ray pulsars) as well as in the non-central heavy ion collisions (HIC), generated along the perpendicular direction of the reaction plane by the fast-moving and positively-charged protons of the colliding nuclei. Initial strength of this magnetic field produced in non-central HIC can be as high as $eB \sim m_\pi^2$ at RHIC energies and $eB \sim 10m_\pi^2$ at LHC energies [2].

The presence of this strong and anisotropic magnetic field can influence the dynamical evolution of heavy quarks (HQ), which serves as an important probe for the properties of quark matter. HQs, with their relative large mass, are generated at the early stage of the initial hard scatterings and subsequently traverse through the fireball experiencing drag forces as well as random "kicks" from the thermal partons in the bulk medium. Hence Langevin equations are widely used for describing HQ in-medium evolution where the essential theoretical inputs include the HQ momentum diffusion coefficients. In absence of eB, several efforts have been made to compute these HQ transport coefficients [3–6]. Though working within the static limit (when HQ is considered to be static because of its much heavier mass) is simpler, going beyond the static limit is needed in light of the current HIC measurements where the transverse momentum scale could be much larger than the HQ masses.

*e-mail: a.bandyopadhyay@thphys.uni-heidelberg.de

In presence of eB also, HQ dynamics have been explored both within and beyond the static limit in some recent studies [7, 8]. Most of those studies are done within the Lowest-Landau-Level (LLL) approximation (i.e. $eB \gg T^2$). HQ mass (M) being the largest scale of the system, the resulting scale hierarchy becomes $M \gg \sqrt{eB} \gg T$. To neglect the soft self energy corrections of the LLL quarks and gluons while evaluating the scattering rate, we also work within a further constraint $\alpha_s eB \ll T^2$, α_s being the strong coupling. Because of the anisotropic nature of the external magnetic field, even when HQ is assumed to be at rest, there will be two momentum diffusion coefficients, i.e. along the longitudinal and transverse directions of the magnetic field. Hence beyond the static limit we will have nontrivial interplay between the directions of eB and HQ velocity, making the problem even more complex and challenging, which we address in this proceeding.

The rest of this proceeding is organized as follows. In section 2 we discuss the basic formalism required to study the HQ dynamics beyond the static limit including the procedure to compute the scattering rate. The following section (section 3) contains our results and corresponding discussions. Finally we summarize and conclude in section 4.

2 Formalism

In the present work the HQ is assumed to be relativistic (i.e. beyond the static limit) in presence of a hot and magnetized medium. We start the current section by discussing the working formulae for the momentum diffusion coefficients in two different cases and gradually move to the computation of the corresponding scattering rate.

2.1 HQ dynamics with magnetic field

The interaction of the HQ with the medium can be approximated as multiple uncorrelated momentum kicks. These uncorrelated momentum kicks can be connected with the scattering process of thermally populated light quarks (q)/ gluons (g) with the heavy quark (H), i.e. $2 \leftrightarrow 2$ scattering processes $qH \to qH$ and $gH \to gH$. At the leading Order of the strong coupling, these scatterings are mediated by one-gluon exchange (Fig. 1), where the participants can be considered as quasiparticles in thermally equilibrated matter. In the rest frame of the plasma, both the $qH \to qH$ and $gH \to gH$ processes predominantly occur only by the t-channel gluon exchange. Hence the momentum diffusion coefficients are directly related to the scattering/interaction rate Γ of the t-channel gluon exchange as

$$\kappa_i = \int d^3q \, \frac{d\Gamma}{d^3q} \, q_i^2, \tag{1}$$

where i can take various values depending on the system. Considering an external magnetic field $\vec{B}$ and a finite velocity $\vec{v} = \vec{p}/E$, we now have two anisotropic directions in the pictures which can be simplified through two cases, as we discuss below.

2.1.1 case 1: $\vec{v} \parallel \vec{B}$

Here the magnetic field and the heavy quark are considered to be moving in similar direction, i.e. z direction for our case. Hence the HQ transverse and longitudinal momentum diffusion coefficients are respectively :

$$\kappa_T(p) = \frac{1}{2} \int d^3q \frac{d\,\Gamma(v)}{d^3q} q_\perp^2, \tag{2a}$$

$$\kappa_L(p) = \int d^3q \frac{d\,\Gamma(v)}{d^3q} q_z^2. \tag{2b}$$

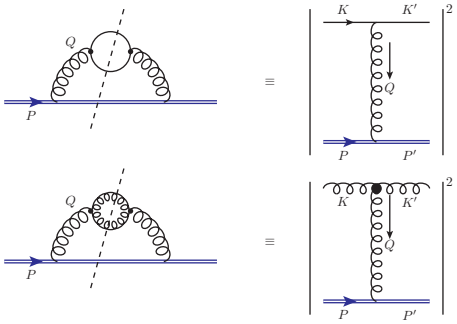

Figure 1. Here we have shown the equivalence of the t-channel scattering of heavy quarks due to thermally generated light quarks and gluons, $qH \to qH$ (left) and $gH \to gH$ (right). The scatterings can also be expressed as the cut (imaginary) part of the HQ self energy.

2.1.2 case 2 : $\vec{v} \perp \vec{B}$

For the second case considered in our present work, the HQ moves perpendicular to (i.e. x or y) the direction of $\vec{B}$ (i.e. z). Because of two anisotropic directions, here we have three momentum diffusion coefficients (i.e. $\kappa_1, \kappa_2, \kappa_3$), respectively given as :

$$\kappa_1(p) = \int d^3q \frac{d\,\Gamma(v)}{d^3q} q_x^2, \tag{3a}$$

$$\kappa_2(p) = \int d^3q \frac{d\,\Gamma(v)}{d^3q} q_y^2, \tag{3b}$$

$$\kappa_3(p) = \int d^3q \frac{d\,\Gamma(v)}{d^3q} q_z^2. \tag{3c}$$

2.2 Computation of the Scattering rate (Γ)

As we have seen in the previous subsection that all the momentum diffusion coefficients in various situations are explicitly dependent on the scattering rate, we now discuss the computation of the same. In this proceeding we will just sketch the basic steps. For the detailed calculation with explicit expression for each step (both for $B = 0$ and $B \neq 0$ case) interested readers can look up in Ref [9].

The scattering rate can be effectively expressed in terms of the cut/imaginary part of the HQ self energy $\Sigma(P)$ [10] as :

$$\Gamma(P \equiv E, \vec{v}) = -\frac{1}{2E} \frac{1}{1 + e^{-E/T}} \text{ Tr}\left[(\not{P} + M)\, \text{Im}\Sigma(p_0 + i\epsilon, \vec{p})\right]. \tag{4}$$

The scattering rate $\Gamma(P)$ has both hard and soft contributions depending on the momentum Q flowing through the gluon line. The hard contribution of $\Gamma(P)$ comes from cutting the two-loop self energy diagrams shown in Fig. 1. The soft contributions are included through the hard thermal loop corrections to the gluon propagator at leading order in g, incorporating resummation in the process. So, instead of two separate processes (i.e. $qH \to qH$ and $gH \to$

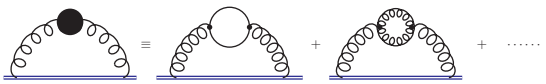

Figure 2. Heavy quark self-energy with effective gluon propagator. Resummation takes into account the diagrams for the hard process (Fig.1) among others.

gH) shown in Fig. 1, we can use an effective resummed gluon propagator (demonstrated in Fig. 2).

In presence of a finite magnetic field, the scale hierarchy in Hard Thermal Loop (HTL) technique becomes more complicated due to the new $\sqrt{eB}$ scale. In our present study, we consider $\{T, \sqrt{eB}\}$ as hard scales for the loop momenta and gT as the soft scale for the external momenta. If one looks at the effective gluon propagator (Fig.2): for the quark/gluon loop there will be the temperature T scale and additionally the $\sqrt{eB}$ scale will come in via the Lowest Landau Level for quarks as the hard scales. The external momentum in gluon propagator is considered to be soft scale gT as usually done in HTL. These scales respect a hierarchy of $gT \ll T \ll \sqrt{eB}$. Hence the effective heavy quark self energy in a magnetized medium is given by,

$$\Sigma(P) = ig^2 \int \frac{d^4Q}{(2\pi)^4} \mathcal{D}^{\mu\nu}(Q)\gamma_\mu S^s_m(P-Q)\gamma_\nu. \tag{5}$$

Here $\mathcal{D}^{\mu\nu}(Q)$ is the gluonic propagator in amganetized medium. On the other hand $S^s_m(P - Q \equiv K)$ is the fermion propagator within the LLL approximation, given as [11, 12],

$$iS^s_m(K) = ie^{-k_\perp^2/|q_f B|} \frac{\not{K}_\parallel + M}{K_\parallel^2 - M^2}(1 - i\gamma_1\gamma_2), \tag{6}$$

with q_f being the fermionic charge for flavor f and $K \equiv (K_\parallel, k_\perp)$ as the fermionic four momentum (Details about these notations can be found in Ref [9]).

Coming to the gluonic propagator at finite temperature and in presence of an external magnetic field, there are several recent studies which construct the general structure of the two point correlation function and differ in their approach by their choice of the independent tensor structures. For the present work we have chosen the effective gluon propagator in a hot and magnetized medium from Ref [13], i.e.,

$$\mathcal{D}^{\mu\nu}(Q) = \frac{\xi Q^\mu Q^\nu}{Q^4} + \frac{(Q^2 - d_3)\Delta_1^{\mu\nu}}{(Q^2 - d_1)(Q^2 - d_3) - d_4^2} + \frac{\Delta_2^{\mu\nu}}{Q^2 - d_2} + \frac{(Q^2 - d_1)\Delta_3^{\mu\nu}}{(Q^2 - d_1)(Q^2 - d_3) - d_4^2} + \frac{d_4\Delta_4^{\mu\nu}}{(Q^2 - d_1)(Q^2 - d_3) - d_4^2}, \tag{7}$$

with the form factors $d_i(Q) = \Delta_i^{\mu\nu}\Pi_{\mu\nu}(Q)$ for $i = 1, 2, 3$ and $d_4(Q) = \frac{1}{2}\Delta_4^{\mu\nu}\Pi_{\mu\nu}(Q)$. $\Delta_i^{\mu\nu}$ are the independent tensor structures, chosen as :

$$\Delta_1^{\mu\nu} = \frac{1}{\bar{u}^2}\bar{u}^\mu\bar{u}^\nu, \tag{8a}$$

$$\Delta_2^{\mu\nu} = g_\perp^{\mu\nu} - \frac{Q_\perp^\mu Q_\perp^\nu}{Q_\perp^2}, \tag{8b}$$

$$\Delta_3^{\mu\nu} = \frac{\bar{n}^\mu\bar{n}^\nu}{\bar{n}^2}, \tag{8c}$$

$$\Delta_4^{\mu\nu} = \frac{\bar{u}^\mu\bar{n}^\nu + \bar{u}^\nu\bar{n}^\mu}{\sqrt{\bar{u}^2}\sqrt{\bar{n}^2}}. \tag{8d}$$

Here u^μ is the heat bath velocity and n^μ is an anisotropic four vector defined uniquely as the projection of the electromagnetic field tensor $F^{\mu\nu}$ along u^μ. Also $\Pi_{\mu\nu}(Q)$ is the gluon self energy in a strongly magnetized medium (within LLL and HTL approximation) : a combination of the eB independent pure glue contribution $\Pi_{\mu\nu}^g$ and eB dependent fermionic loop contribution $\Pi_{\mu\nu}^s$. Again, for the details about the construction of the tensor structure and the notations of $\bar{u}^\mu, \bar{n}^\nu, g_\perp^{\mu\nu}, \Pi_{\mu\nu}^s, \Pi_{\mu\nu}^g$ etc., interested readers can look up in Refs [9, 13].

So, using Eqs. (5), (6) and (7) in Eq. (4) and evaluating the following traces, imaginary contributions and frequency sums one can get the final simplified expression for the scattering rate $\Gamma(P)$ for a relativistic HQ moving in a hot magnetized medium. After getting the expression for the $\Gamma(P)$, it is fairly straightforward to obtain the corresponding expressions for the momentum diffusion coefficients κ_i's for both the cases $\vec{v} \parallel \vec{B}$ and $\vec{v} \perp \vec{B}$. The final expressions for both the cases are given in Ref. [9]. Finally to reach the relatively well known static limit results for the momentum diffusion coefficients, one can take the $\vec{v} \to 0$ limit in our general expressions.

3 Results

In the following subsections we discuss our findings for different momentum diffusion coefficients (in two different scenarios) for charm and bottom quarks moving through a strongly magnetized hot medium.

3.1 case 1 : $\vec{v} \parallel \vec{B}$

In this case we have one anisotropic direction, vis-a-vis two different momentum coefficients : κ_L and κ_T, representating the longitudinal and transverse components respectively. The heavy quark momentum is only nonzero in the $\vec{B}$ direction, i.e. $p \equiv p_z$. The charm and bottom quark masses are taken to be $M = 1.28$ GeV and $M = 4.18$ GeV respectively, moving parallel to an external magnetic field along the z direction. We have chosen the HQ momentum p to be 1 GeV to maintain the scale hierarchy of $M \gg p \gg T$ which we consistently used to simplify our expressions. Choosing a relatively high value of 1 GeV for the HQ momentum also solidifies our claim of going beyond the static limit. We also compare our finite eB results with the $eB = 0$ results obtained from Ref. [6]. For the same, we have chosen the Ultra-Violate (UV) cut-off as $q_{max} = 3.1Tg(T)^{1/3}$, as discussed in Ref. [6]. For finite eB calculations, an UV cut-off like q_{max} is not necessary because of the presence of the $e^{-k_\perp^2/|q_f B|}$ factor appearing from the fermion propagator in a magnetized medium.

In Fig. 3 we present two different plots for charm (left panel) and bottom (right panel) quarks. Each plot shows the coefficients κ_L (solid lines) and κ_T (dashed lines) together. For

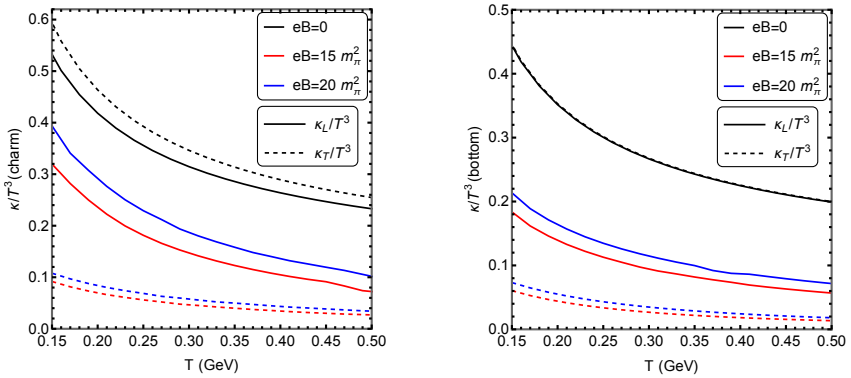

Figure 3. Variation of the scaled κ_L (solid lines) and κ_T (dashed lines) with temperature for three different values of external magnetic field, i.e. $eB = 0, 15m_\pi^2, 20m_\pi^2$ and for both charm (left panel) and bottom (right panel) quarks, considering $\vec{v} \parallel \vec{B}$. Charm and bottom quark masses M and HQ momentum p are specified in the text.

increasing magnetic field, one can observe enhancements in both the longitudinal and transverse components of the momentum diffusion coefficients. Although in comparison with the $eB = 0$ case, the values for κ_L and κ_T appear to be significantly reduced by finite magnetic fields, for both charm and bottom quarks. We also observe that for finite eB, values of κ_L are significantly higher than κ_T, unlike the $eB = 0$ case, where $\kappa_T > \kappa_L$ for charm quark (left panel) and κ_L and κ_T fall on top of each other for bottom quark (right panel).

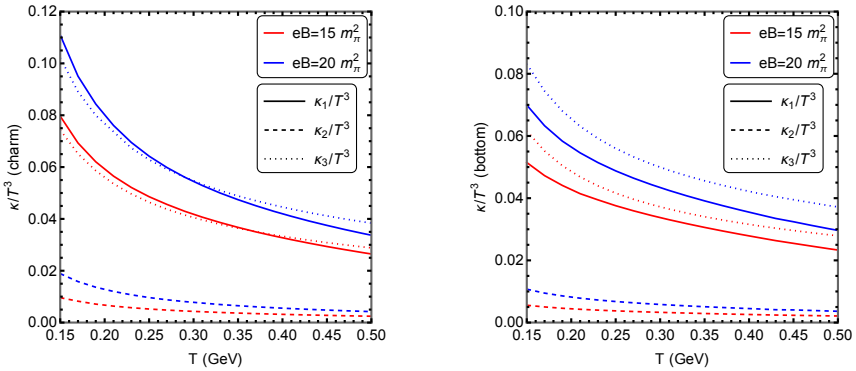

Figure 4. Variation of the scaled charm (left panel) and bottom (right panel) quark momentum diffusion coefficients (i.e. κ_1, κ_2, κ_3 for $\vec{v} \perp \vec{B}$ represented respectively by solid, dashed and dotted lines) with temperature for two different values of external magnetic fields, i.e. $eB = 15m_\pi^2$ and $20m_\pi^2$. Charm and bottom quark masses M and HQ momentum p are specified in the text.

3.2 case 2 : $\vec{v} \perp \vec{B}$

For our second case, we have two anisotropic directions given by $\vec{v}$ and $\vec{B}$, which generate three different momentum coefficients, which we have noted as κ_1, κ_2 and κ_3. One can think

κ_3 as the longitudinal component and $\{\kappa_1, \kappa_2\}$ as the transverse components. In this case the heavy quark momenta can be nonzero in x and/or y direction. For our purpose the heavy quark is chosen to be moving along the x direction, i.e. $p \equiv p_x$. Since this scenario is exclusive for finite eB, we do not compare the $eB = 0$ result here.

In Fig. 4 we have presented two separate plots for the charm (left panel) and bottom (right panel) quarks. For both the cases we have shown the variations for scaled transverse components κ_1, κ_2 and longitudinal component κ_3. From the plots for bottom quarks one can notice that the longitudinal component κ_3 (dotted lines) values are the largest, followed by the transverse component κ_1 (solid lines) values. For charm quarks though, a crossover is observed between κ_1 and κ_3, where the former dominates at lower T and the latter at higher T. As a consequence of our choice of HQ movement along the x direction, values of κ_2 (dashed lines), which is basically transverse to both the magnetic field and the velocity directions, appear to be the lowest of the plot, almost an order of magnitude lower than κ_1/κ_3. Similar to the previous case, here also, with an increasing magnetic field, values for all the HQ momentum diffusion components have increased.

4 Summary

In summary, the present proceeding highlights our recent study of the momentum diffusion coefficients for heavy quarks (charm and bottom) moving in a hot and strongly magnetized quark-gluon plasma. Two specific cases have been discussed, i.e. HQ moving parallel to the external magnetic field ($\vec{v} \parallel \vec{B}$) and HQ moving perpendicular to the external magnetic field ($\vec{v} \perp \vec{B}$). For these two cases we evaluate the momentum diffusion coefficients within the HTL approximation. Along with the hard contributions, to incorporate the soft contributions in our evaluation we have worked with an effective HTL gluon propagator in a hot and magnetized medium [13]. For $\vec{v} \parallel \vec{B}$, we have two different momentum diffusion coefficients, longitudinal κ_L and transverse κ_T. On the other hand for $\vec{v} \perp \vec{B}$ we have three different momentum diffusion coefficients along three spatial directions, i.e. κ_1, κ_2 and κ_3. For all these κ's, we explore the temperature variations for different values of eB. Both for charm and bottom quarks these observations revealed some interesting features. Numerical evaluations also demonstrate a considerable influence of the strong magnetic field on these coefficients for eB values accessible in high energy HIC. Going beyond the LLL approximation, adopted in the present work, would be a natural next step forward. It would also be highly interesting to explore the phenomenological implications of these theoretical results. More specifically, there could be nontrivial consequences of the anisotropic momentum diffusion coefficients due to the magnetic field for experimental observables such as directed and elliptic flow of the open heavy flavor mesons.

5 Acknowledgments

This work is supported in part by the Guangdong Major Project of Basic and Applied Basic Research No. 2020B0301030008, Science and Technology Program of Guangzhou Project No. 2019050001, the National Natural Science Foundation of China under Grant No. 12022512, No. 12035007, No. 11735007, as well as by the NSF Grant No. PHY-2209183. A.B. acknowledges the support of the postdoctoral research fellowship from the Alexander von Humboldt Foundation, Germany.

References

[1] S. Chakrabarty, D. Bandyopadhyay, S. Pal, Phys. Rev. Lett. **78**, 2898 (1997), astro-ph/9703034

[2] V. Skokov, A.Y. Illarionov, V. Toneev, Int. J. Mod. Phys. A **24**, 5925 (2009), 0907.1396
[3] G.D. Moore, D. Teaney, Phys. Rev. C **71**, 064904 (2005), hep-ph/0412346
[4] S. Caron-Huot, G.D. Moore, Phys. Rev. Lett. **100**, 052301 (2008), 0708.4232
[5] S. Caron-Huot, G.D. Moore, JHEP **02**, 081 (2008), 0801.2173
[6] A. Beraudo, A. De Pace, W.M. Alberico, A. Molinari, Nucl. Phys. A **831**, 59 (2009), 0902.0741
[7] K. Fukushima, K. Hattori, H.U. Yee, Y. Yin, Phys. Rev. D **93**, 074028 (2016), 1512.03689
[8] M. Kurian, S.K. Das, V. Chandra, Phys. Rev. D **100**, 074003 (2019), 1907.09556
[9] A. Bandyopadhyay, J. Liao, H. Xing, Phys. Rev. D **105**, 114049 (2022), 2105.02167
[10] H.A. Weldon, Phys. Rev. D **28**, 2007 (1983)
[11] J.S. Schwinger, Phys. Rev. **82**, 664 (1951)
[12] V.P. Gusynin, V.A. Miransky, I.A. Shovkovy, Nucl. Phys. B **462**, 249 (1996), hep-ph/9509320
[13] B. Karmakar, A. Bandyopadhyay, N. Haque, M.G. Mustafa, Eur. Phys. J. C **79**, 658 (2019), 1804.11336